YAP/TEAD involvement in resistance to paclitaxel chemotherapy in lung cancer

Solenn Brosseau
U830 INSERM "Cancer, Institut Curie Research Centre
Paula Abreu
U830 INSERM "Cancer, Institut Curie Research Centre
Clémentine Bouchez
U830 INSERM "Cancer, Institut Curie Research Centre
Lucie Charon
U830 INSERM "Cancer, Institut Curie Research Centre
Yann Kieffer
U830 INSERM "Cancer, Institut Curie Research Centre
Géraldine Gentric
U830 INSERM "Cancer, Institut Curie Research Centre
Valentin Picant
U830 INSERM "Cancer, Institut Curie Research Centre
Irina Veith
U830 INSERM "Cancer, Institut Curie Research Centre
Jacques Camonis
U830 INSERM "Cancer, Institut Curie Research Centre
Stéphanie Descroix
CNRS "Physics and Chemistry Curie" Institut Curie Research Centre
Fatima Mechta-Grigoriou
U830 INSERM "Cancer, Institut Curie Research Centre
Maria-Carla Parrain
U830 INSERM "Cancer, Institut Curie Research Centre
Gérard Zalcman (✉ gerard.zalcman@aphp.fr)
Université Paris Cité

Research Article

Keywords: lung cancer, YAP (yes-associated protein), TEAD, microfluidics, chemo-resistance, paclitaxel

Posted Date: September 25th, 2023

DOI: https://doi.org/10.21203/rs.3.rs-3363457/v1

Abstract

Background: The Yes-associated protein (YAP) oncoprotein has been linked to both metastasis and resistance to targeted therapy of lung cancer cells. We aimed to investigate the effect of YAP pharmacological inhibition, using YAP/ TEA domain (TEAD) transcription factor interaction inhibitors, in chemo-resistant lung cancer cells.

Methods: YAP subcellular localization, cell migration, and TEAD transcription factor functional transcriptional activity were investigated in cancer cell lines with up-regulated YAP, with and without YAP/TEAD interaction inhibitors. Parental (A549) and paclitaxel-resistant (A549R) cell transcriptomes were analyzed. The half-maximal inhibitory concentration (IC_{50}) of paclitaxel or trametinib, an inhibitor of Mitogen-Activated protein kinase and Erk Kinase (MEK), combined to YAP/TEAD inhibitor (IV#6) was determined. A three-dimensional (3D) microfluidic culture device enabled us to study the effect of IV#6/paclitaxel combination on cancer cells isolated from fresh resected lung cancer samples.

Results: YAP activity was significantly higher in paclitaxel-resistant cell lines. YAP/TEAD inhibitor induced a decreased YAP activity in A549, PC9, and H2052 cells, with reduced YAP nuclear staining. Wound healing assays upon YAP inhibition revealed impaired cell motility of lung cancer A549 and mesothelioma H2052 cells. Combining YAP pharmacological inhibition with trametinib, in A549, K-Ras mutated cells, recaped synthetic lethality, sensitizing these cells (MEK) inhibition. The YAP/TEAD inhibitor lowered paclitaxel IC_{50} in A549R cells. Differential transcriptomic analysis of parental and A549R cells revealed an increase of YAP/TEAD transcriptomic signature in resistant cells, down-regulated upon YAP inhibition. YAP/TEAD inhibitor enabled restoring paclitaxel sensitivity in A549R cells cultured in a 3D microfluidic system, with lung cancer cells from a fresh tumor efficiently killed by YAP/TEAD inhibitor/paclitaxel doublet.

Conclusions: Evidence on YAP/TEAD transcriptional program's role in resistance to chemotherapy opens routes towards therapeutic YAP targeting.

Background

Lung cancer remains the leading cause of cancer-related deaths worldwide with almost 1.8 millions of deaths per year (1). Remarkable efforts have been made worldwide to understand the molecular basis for such lung cancer aggressiveness, especially concerning non-small cell lung cancer (NSCLC), allowing for developing targeted therapies for cancers with oncogenic addiction, or immunotherapy for tumors without addictive targetable mutations. However, chemotherapy remains the backbone treatment for NSCLC patients, either associated with immunotherapy for patients with not-addicted tumors, or administered in subsequent lines setting, for patients with tumors containing an oncogenic addictive mutation that progress under frontline tyrosine kinase inhibitors. Despite recent advances, patients with metastatic NSCLC still experience a dismal prognosis. Poor overall survival could be attributed, at least to some extent, to the drug resistance development. Only few genetic (selection of pre-existing genetic

variants), and non-genetic (up-regulated expression of the therapeutic target, activation of compensatory pathways…etc.) mechanisms have been identified to date, through which cancer cells develop drug resistance (2). Paclitaxel is a widely used anti-microtubule agent for treating lung cancer patients. Nevertheless, acquired resistance to such agent is common, with patients ultimately experiencing disease progression and metastasis emergence. The mechanisms of chemo-resistance have been extensively studied but biological mechanistic processes remain elusive (3–6).

Initially discovered in *Drosophila Melanogaster* for its role in the control of development and organs size, Hippo signaling pathway has been conserved throughout evolution from drosophila to mammals, emphasizing its major role in tissue homeostasis (7). Once activated, core serine threonine kinases of this cascade, including Mammalian Sterile 20-like kinase (MST) 1 (aka 'Hippo' in drosophila) and 2, as well as Large Tumor Suppressor (LATS) 1 and 2 ('Warts' in drosophila) induce phosphorylation of final downstream effectors, the paralogs Yes-associated protein (YAP) and Transcriptional co-activator with PDZ-binding motif (TAZ). Such serine phosphorylation inactivate YAP/TAZ which could then be sequestered within the cytoplasm by interacting with the 14-3-3 chaperones, or being targeted to proteasome degradation via ubiquitinylation (8). YAP/TAZ act as transcriptional co-regulators, by interacting with DNA-binding transcription factors (mainly TEAD1-4 genes, *i.e.* TEA Domain Transcription Factors), to modulate the mRNA expression of genes involved in cell proliferation, survival, migration and stemness (9). YAP was found to act as a powerful oncogene in several cancers, especially NSCLC, increased YAP levels correlating with poor prognosis (10). Upstream negative regulators of such pathway consist of tumor suppressor genes, which are often inactivated by either mutation (NF2/Merlin in mesothelioma), or promoter gene methylation (RASSF1A in NSCLC) (11), inducing YAP-mediated transcriptional activity up-regulation. Several studies suggested that the Hippo/YAP pathway deregulation could contribute to anti-cancer drug resistance in solid tumors (2, 12). Recently, drugs that directly (like Verteporin), or indirectly (like statins), target the Hippo signaling pathway were investigated for their ability to overcome cancer cells' drug resistance (13, 14). Nevertheless, for relevant YAP inhibition, high doses were required, resulting in predictable side-effects, limiting their clinical utility (13). Lately, inhibitors able to bind the interaction surface of TEAD with YAP, were rationally synthetized, based on the three-dimensional structure of the two protein complexes, that target a palmitate consensus cysteine on TEAD, which is palmitoylated. These inhibitors were associated with YAP/TEAD transcriptional inhibitory ability, thereby inducing tumor regression in mice xenografted tumors, derived from cells with up-regulated YAP signaling (mutation of NF2). Such first-generation YAP/TEAD inhibitors were active at 10µM range or more, thus limiting their clinical applicability. However, a second-generation drug with 500nM activity (IK-930, by Ikena Oncology™), is currently undergoing investigation in a first-in human phase I trial. Other YAP inhibitors have been isolated from large interaction screens, by different pharmaceutical companies, currently undergoing preclinical development. We were supplied with such compounds by Inventiva™ BiotechPharma, and thus able to assess their biological efficacy in inhibiting YAP/TEAD activity, using several biological assays. We first sought to assess their efficacy in limiting NSCLC cells migration, having previously reported that RASSF1A inhibition could increase cancer cell migration by activating YAP (15). We then aimed investigated whether such inhibitors could alter cancer

cells sensitivity to the anti-tubulin agent, paclitaxel, having previously reported that RASSF1A depletion and YAP activation could impair cytokinesis in link with deregulation of microtubules (16)

Given that *in vitro* 2D cell cultures have been challenged concerning their ability to faithfully recap *in vivo* drug sensitivity, we employed a micro-fluidic 3D cell culture experimental system, in which cells are grown embedded in a polymerized collagen matrix, aimed at reconstituting *in vitro*, either with cell lines, or directly with human cells from fresh tumors, a more physiological culture system, which was prone to better recapitulate *ex-vivo* cytotoxic drug cancer cell sensitivity (17–19). To the best of our knowledge, we were the first to use such system to assess YAP inhibitor activity on cell growth and apoptosis, the inhibitor being given either alone or in combination with paclitaxel. Herein, we have presented *in vitro* and *ex-vivo* studies that assessed the effects of YAP/TEAD pharmacological inhibition on cell migration, YAP nuclear cellular localization, synthetic lethal activity in K-Ras mutated cells, and re-sensitization of drug-resistant lung cancer cells towards paclitaxel, using classical 2D cell cultures, and a microfluidic 3D cell culture experimental device.

Methods

Cell lines and culture reagents. Parental lung adenocarcinoma cell lines A549 (CRL-185) and HCC827 (CRL-2868) were obtained from Kent University Resistant Cancer Cell Line (RCCL) collection, with their counterpart sub-clones A549R and HCC827R, resistant to paclitaxel after long-term cultures with 20 nM of paclitaxel. Mesothelioma sarcomatoid cell line H2052 with constitutive YAP activation (20), and Met5A SV40-immortalized, non-tumorigenic human mesothelial epithelioid cell line, were obtained from ATCC (CRL-5915, and CRL-9444 respectively), and passaged for fewer than six months after their receipt. PC-9 (CRL-1520) and HCC4006 (CRL-2871) lung adenocarcinoma cell lines from ATCC both contained an EGFR mutation (exon 19 deletion). All cell lines were STR genotyped to check their identity (15). Cells were maintained in RPMI-1640 (Roswell Park Memorial Institute) medium with 10% fetal bovine serum (FBS), 10mM L-Glutamine, and 1% penicillin/streptomycin (Invitrogen™).

Compounds. First-generation YAP-TEAD inhibitors, (IV#1, IV#2, IV#3, IV#4, IV#5, IV#6), were provided by Inventiva™ Pharma Company (Daix, France), having significant activity in a TEAD- mediated YAP transactivation assay. IC_{50} values with such assay for these compounds ranged from 0.2 µM to 7.3 µM with maximal inhibition ranging from 79–95% (22). Trametinib was purchased from Sellekchem™ (Houston, TX, USA) and Paclitaxel from Fresenius Kabi™ (Bad Homburg, Germany). All drugs were diluted in DMSO.

Wound healing assay. Culture-Inserts (Ibidi™) were used to measure cell migration. Cell suspension at a density of 6×10^4/mL (70 µL volume) was plated in each well of the Culture- Inserts for 2 h in DMEM medium with 1% fetal bovine serum (FBS). The cells were then treated with YAP-TEAD interaction inhibitors (20 µM). A cell-free 500µm gap was created by removing the Culture-Insert. Images were captured every 15 minutes for 48 hours using an inverted phase-contrast automated video-microscope. The velocity of cell migration in three randomly chosen fields was calculated with AveMap freeware (23).

TGFβ-induced epithelial to mesenchymal transition

Recombinant TGFβ1 (R&D Systems™) was added in the culture medium at 2ng/ml concentration for 24 hours to induce epithelial to mesenchymal transition (EMT). For western-blot analysis, N-cadherin (cat#14215) and E-cadherin (cat# 94385) antibodies were purchased from Cell Signaling Technology™ (Danvers MA, USA). YAP/TEAD inhibitors were used at 20 μM concentration for 48 hours.

Immunofluorescence. Cells were plated on coverslips 24 hours before drug treatment at the concentration of 5 x 10^4 cells, to limit cell confluence. A549 and HCC827 cell lines were incubated with 10 μM and 5 μM IV#6 respectively, for 24 hours. Each well containing inhibitor compound was paired with a control well, containing DMSO. Cells were fixed and permealized (15). Slides were then incubated with the primary antibody (rabbit Antibody, YAP cat#D8H1X, Cell Signaling, dilution 1:100), and secondary antibody (goat anti-rabbit Antibody, AlexaFluor488 InVitrogen™, dilution 1:1000), plus phalloïdin (InVitrogen™, dilution 1:500) for one hour in PBS buffer solution. Nuclei were counter-colored with Prolong (InVitrogen™) containing DAPI. Image J software allowed for immunofluorescence quantification in the nucleus and cytoplasm of 150 cells per condition, and the ratios of nuclear to cytoplasm YAP being then calculated.

IC50 experiments. A549 cell lines were seeded at 10,000 cells density per well in 50ul culture medium, in 96 well culture plates. The next day, drugs were added at different concentrations in triplicates: 25μl of anti-YAP/TEAD compound at 10μM and 25μl of paclitaxel-containing medium at varying concentrations (0.01nM, 0.1nM, 1nM, 10nM, 100nM, 1μg, 10μg, 100μg). After 3 drug treatment days, the cell viability was assessed using the Cell Titer-Glo 2.0 Cell Viability Assay™ (Promega™, Madison, WI, USA), based on the manufacturer's instructions. Using Grad Pad PRISM™ 9 software, the inhibitor IC50 was measured as the concentration that causes a response halfway between the maximum response (top) and the maximum inhibited response (bottom).

Short interfering RNA (si RNA): Cells were transfected with 10nM siRNA in a petri dish plate. Control was non-targeting siRNA (SinT, AllStars negative control, cat#1027281) and the YAP1 silencing was obtained with YAP1 targeting siRNAs (YAP si1: 5'-TGA-GAA-CAA-TGA-CGA-CCA-A-3' and YAP si2; 5'-TTG-GTC-GTC-ATT-GTT-CTC-A-3'). Transfection reagent was lipofectamine RNAiMAX (Invitrogen™, Carlsbad, CA, USA). 10,000 cells per well (96-well plate) were seeded, 24 hours after transfection. The IC50 was determined 3 days after drug addition.

Protein extraction and Western Blot

Protein Extraction

After addition of 120μl of IPLB lysis buffer containing Complete Protease Inhibitors, EDTA free (Roche Pharma™, Basel, CH), cells were collected, incubated 20 min on ice, then sonicated for 10 min and centrifuged for 10min at 13,000 rpm and 4°C.

Western Blot

Cells proteins were heat-denaturated for 5 minutes at 95°C, resolved in NuPAGE™ Novex 4–12% Bis-Tris midi protein gel (Invitrogen™) and electro-transferred onto a 0.45µm nitrocellulose membrane (Amersham Protran™ 0.45um, GE Healthcare Life Sciences™, Marlborough, MA, USA). The membrane was probed overnight at 4°C with YAP Rabbit monoclonal Ab (D8H1X) XP® (#14074, Cell Signaling, Danvers, MA, USA). The next day, incubation with the secondary antibody was performed for 1 hour at room temperature, with detection of immunoreactive bands achieved using ECL 1.1 (Western Lightning Plus ECL™, PerkinElmer™, Waltham, MA, USA). Immunoblots were scanned with Chemidoc™ imaging system (Bio-Rad, Hercules, CA, USA), and protein bands analyzed using ImageJ™ software for protein quantification.

Dual Luciferase Assay

Cells (3 x 10^6) were transfected with a reporter plasmid containing the minimal promoter sequences of TEAD upstream of the gene encoding for firefly luciferase (firefly plasmid, 6µg, pGL3b 8xGTIIC TEAD) and with a normalizing plasmid containing a constitutive expression promoter (Renilla lpRL-TK plasmid, 0.02 µg, from Promega™, Madison, WI, USA) in Jet Prime Buffer and Reagent solution (Polyplus transfection™). Twenty-four hours after transfection, cells were washed (PBS 1X), detached (trypsine) and plated in 6-well plates at different concentrations (25 x 10^3, 1 x 10^5, 4 x 10^5, 8 x 10^5, 1.2 x 10^6) to obtain different levels of confluence. The YAP/TEAD interaction inhibitor IV#6 was added in the media at least 4 hours after plating, for 24 hours, at 10 µM for A549 cell line (n = 10) and 5 µM for HCC827 cell line (n = 7). Cells were washed (PBS 1X) and lysed (Passive Lysis Buffer 1X, Promega™), 48 hours maximum after transfection in 96-well plates, and luminescence quantified (Optima FLUOSTAR™) with a bioluminescence counter with two reagents (Luciferase Assay Reagent II and Stop&Glo Reagent, Promega™). The firefly/renilla luminescence ratio was measured for each cell line at different confluences.

RNA sequencing analysis

Parental and resistant A549 cells (3 x 10^6) were seeded and grown up to 50% confluence. The YAP-TEAD interaction inhibitor IV#6 was added in the media for 24 hours. Cell lysis was performed with 750 µL of Qiazol™, the lysis solution being frozen at -80°C. This step was repeated three times, with two passages interval (n = 3). Total RNA was extracted using miRNAeasy MiniKit (Qiagen™, Germantown, MD, USA). RNA concentration was assessed by a NanoDrop™ spectrophotometer. A minimum of 2 µg of RNA was required. RNA integrity and quality were analyzed using Agilent RNA 6000 Nano Kit (Agilent Technologies™, Santa Clara, CA, USA). All samples with a RIN score > 7.5 were sent to the Institut Curie central lab facility for RNA sequencing. cDNA library was prepared using Nextera XT sample preparation kit, followed by sequencing on NovaSeq (Illumina) paired-end 100. Reads were mapped on the human genome assembly GRCh38 (hg38) and quantified using STAR (version 2.6.1A). Only genes with reads in at least 5% of all samples were kept for further analyses. Normalization and differential analysis were conducted with DESeq2 R package. Principal Component Analysis was generated from variance stabilized normalized counts table on the 1000 most variables gens.

3D-culture on-chip

The experimental micro-fluidic system aiming at reconstituting *in vitro* with the cell lines, or *ex-vivo* from human cells directly isolated from fresh tumors, a 3D microenvironment on a chip, *i.e.* a "cancer-on-chip" system, was previously described (18, 24). The microfluidic chips (#DAX-1) were purchased from AIM-Biotech™ (Singapore, Singapore). Within the central chamber of the DAX-1 chip, A549 cells were seeded at a concentration of 2 x 10^6 cells / mL in a matrix composed of type I rat tail collagen (Thermofisher Scientific™) at 2.3 mg/mL final concentration. The collagen solution polymerisation was achieved by 30 min incubation at 37˚C in a humidified chamber. Then, 120 µL of culture medium with different drug conditions (Paclitaxel, IV#6) were added in each lateral chamber. After the medium was added, the microfluidic devices transferred to the incubating chamber of the microscope for video-imaging (Fig. 8A).

Before seeding in the gel, cancer cells were detached, and re-suspended at 10^6 cells/mL density in PBS with 5 µM CellTrace Yellow™ (Thermofisher Scientific™), for living cells detection in the red fluorescence channel. After 5 min incubation in cell medium at 37˚C, cells were centrifuged at 300g for 5 min, re-suspended in PBS and added to the rat-tail collagen solution. CellEvent™ Caspase-3/7 Green Detection Reagent (Thermofisher Scientific™) was added to the media in the lateral chamber of the chip and cell apoptosis visualized in the green fluorescence channel. To detect all-causes cell death rather than cell apoptosis only DRAQ7 dye (Colorant DRAQ7™, Thermofisher Scientific™) was used. The video-microscope was equipped with a CO_2 (5%) and temperature-controlled (37˚C) incubator chamber, saturating humidity being ensured by humidified small sponges added to the chip's surroundings. Time-lapse images were acquired with an inverted Leica DMi8™ equipped with a Retiga R6 camera™ and Lumencor SOLA SE 365™ light engine, with a 5X objective. The image acquisition in transmission and fluorescent channels was performed every hour over 72 h. STAMP software was developed and patented via MATLAB™ to count apoptotic events on the chip for 72 hours according to the "fluorescence switch" from red to green (24).

Cell isolation from fresh tumors

A digestion and negative selection method using MACS Tissue dissociation Kit, (Miltenyi Biotec™. San José, CA, USA) was used as previously described, to recover tumor cells from fresh surgical lung cancer samples (25). After sample digestion with dissociation enzymatic buffer for 45 minutes at 37°C, the tumor lysate was filtered with erythrocytes removed using the Red Blood Cell lysis Solution 10X (Miltenyi Biotec™). Tumor cells were isolated with Tumor cells isolation kit, human Miltenyi Biotec™. Cancer cells were counted with their viability being evaluated using a precise number of cells re-suspended in a previously prepared collagen gel at 4°.

According the French regulatory rules, patients followed-up at Hospital Bichat's Thoracic Oncology Department received an information leaflet, stating that anonymized clinical data would be collected, and that their cancer cells likely to be purified from fresh surgical pathological samples. They were reminded that they could oppose at any time their data and cells utilization for research purpose. The study was

approved by the Institutional French Society of respiratory medicine (*Société de Pneumologie de Langue Française* (SPLF) review board (number #CEPRO 2020-051).

Statistical analyses

Immunofluorescence data were analyzed using GraphPad Prism™ version 9 software (Dotmatics™, San Diego, CA, USA). As they follow a normal distribution, the data were compared using the Student t-test. For IC_{50} data, which did not follow a normal distribution, the Mann-Whitney test was used for comparisons. Firefly/renilla luminescence ratios data did not follow a normal distribution either, and were compared with Wilcoxon test. For transcriptomics analyses, comparison of the YAP/TEAD signature between the different conditions was performed using a Welch two-sample t-test. For all statistical analyses, p-value < 0.05 was set for statistically significant difference. All supporting data will be made available on request to the corresponding author (GZ).

Results

YAP-TEAD interaction inhibitors decrease YAP nuclear localization and cell velocity.

With the objective to investigate the biological effects of different Inventiva™-supplied YAP/TEAD interaction inhibitors compounds, immunofluorescence assays were performed to calculate the intensity ratio between YAP nucleus and cytoplasm staining. These tests were carried out using A549, H2052 and Met5A cell lines, grown at low to moderate density, to avoid any mechano-transduction effect potentially leading to YAP nucleus exit in the event of high cell density (Fig. 1**).** Following treatment, this ratio was significantly lowered in the A549 and H2052 cells, namely two cell lines previously reported to have increased basal YAP activity, owing to STK11 mutation and RASSF1A methylation for the former (15, 16), and NF2 and LATS2 mutation for the latter (20). The effect was particularly marked following IV#6 ($p < 0.0001$, $n = 3$, Student t-test) (Fig. 1, **upper and middle panel**). Conversely, the ratios observed in the Met5A cell line did not support any IV#6 effect in such immortalized, non-tumorigenic cells, without known alteration in the Hippo/YAP pathway (Fig. 1, **lower panel**).

Thereafter, we analyzed the migration speed of A549 and H2052 cells in the presence of two YAP/TEAD interaction inhibitors IV#5 and IV#6 at increasing concentrations (Fig. 2**).** These treatments significantly and dose-dependently decreased the 2D cell velocity. Representative images of the wound healing assay were taken at 0 and 48 hours after cell- free gap creating (Fig. 2**)**, and the velocity (µm/h) was calculated using Avemap™ software, which determines cell velocity, using an image correlation method, without being influenced by cell proliferation (23). The 20µM dose was likely the most efficient dose, resulting in significantly decreased cell migration ($p < 0.0001$, $n = 3$, Student t-test), without any cell toxicity. Accordingly, all other Inventiva™ YAP-TEAD interaction inhibitors reduced cell velocity of both cell lines at 20µM either (**Suppl. Figure 1**), although their effect was more pronounced in H2052 cells, suggesting a higher YAP inhibition susceptibility in these cells, as compared with A549 cells.

YAP-TEAD interaction inhibitors partly revert epithelial to mesenchymal (EMT) transition induced by TGF-β in A549 lung cancer cells.

As previously reported by us (15), along with other authors, YAP signaling activation, by RASSF1A depletion for instance, could induce EMT in epithelial lung cancer cells. A549 cells are already engaged towards a partial EMT, as reflected by low basal N-Cadherin expression levels (**Figure Suppl.2**, **panel A**). This could be further stimulated by TGFβ treatment as shown by the increased N-cadherin expression, with concurrent decrease of E-cadherin (26). Upon YAP pharmacological inhibition with the two most active compounds at 20µM (IV#5 and IV#6), we were able to inhibit N-cadherin expression induced by TGFβ treatment (**Figure Suppl.2**, line 1 **panel B**). Concurrently E-cadherin failed to increase, suggesting that YAP pharmacological inhibition only partly reverted EMT in this lung cancer cell model (**Figure Suppl. 2, panel C** for quantification of four independent experiments). Such results clearly support an actual effect of tested YAP/TEAD inhibitors in disrupting YAP/TEAD interaction, with partial reversibility of TGFβ-induced EMT as a functional consequence.

Anti YAP/TEAD Compounds sensitizes A549 cells to MEK inhibitor

Trevor Bivona's team identified YAP pathway activation as a novel resistance mechanism to kinase inhibitors targeting RAF and MEK therapy, in the presence of B-RAF V600E or K-RAS activating mutations. These authors revealed a synthetic lethality effect induced by RNA interference-mediated depletion of YAP, with simultaneous inhibition of MEK by trametinib, specifically in K-Ras or B-Raf mutated cell lines. Of note such effect was not observed in cells without MAP-K signaling constitutive activation (27). We thus sought to recapitulate this effect using pharmacological compounds targeting YAP/TEAD interaction, in combination with trametinib. This was meant to support their specific effect on YAP downstream signaling in the A549 cell line exhibiting a K-Ras G12S oncogenic mutation, with predominant nuclear YAP staining. For this, we calculated the trametinib IC_{50} in our cancer cells, in the presence of Inventiva™-supplied compounds over 7 days (Fig. 3A). Using pharmacological agents, we recapitulated the synthetic lethality induced in such cells by YAP genetic depletion while combining trametinib with the IV#6 compound. Indeed, the trametinib IC_{50} was significantly reduced by IV#6 at 20µM for 7 days ($p = 0.0432$, Student t-test, $n = 3$). The compounds without trametinib did not exhibit significant toxicity (Fig. 3B). Thereafter, we calculated the trametinib IC_{50} in the presence of YAP SiRNA for three days, prior to the YAP transient knockdown's fading (Fig. 3C). YAP knockdown did not decrease cell viability per se (Fig. 3D**)**. YAP knockdown was maximal over 90% at 3 days (Fig. 3E**)**. Trametinib's pharmacological efficacy was verified in cell extracts by the decreased phospho-ERK band on Western blot (Fig. 3F**)**. As observed with pharmacological inhibition, YAP knockdown actually enhanced trametinib's efficacy on A549 cells ($p < 0.05$, Student's t-test, $n = 3$), as did YAP/TEAD pharmacological inhibitor (Fig. 3C).

Chemo-resistance of paclitaxel-resistant lung cancer cell line correlates with an increase of YAP activity

To compare basal activity of YAP in parental cell lines and their paclitaxel-resistant counterparts, we performed a functional transactivation luciferase reporter assay as described by the S. Piccolo's team (28). The protocol involves two plasmids co-transfection including a reporter plasmid containing TEAD minimal promoter sequences upstream the gene encoding firefly luciferase (Firefly plasmid - pGL3b 8xGTIIC TEAD), as well as a plasmid constitutively expressing renilla luciferase (Renilla lpRL-TK plasmid), to normalize firefly luciferase's enzymatic activity, for overcoming the variation of plasmid's transfection efficiency and transfection-induced cell death. Thus, the bioluminescence is expected to be proportional to the nuclear content of active YAP interacting with nuclear TEAD. YAP activity, measured by the luciferase reporter assay, was revealed to be clearly higher in resistant A549 and HCC827 cells than in their parental counterparts ($p = 0.0082$ for A549 and $p = 0.0014$ for HCC827; $n = 10$ for each cell line; Student-t test) (Fig. 4A).

To further confirm these results, we performed YAP immunofluorescence to compare YAP's localizations among different cell lines. To this end, we calculated the YAP nuclear to cytoplasmic labelling ratio in 150 arbitrarily chosen cells for each condition, ensuring the cell density was low-to-moderate and being comparable. The nuclear to cytoplasm YAP fluorescent signal ratio was significantly higher in the resistant A549 cells ($p < 0.0001$; $n = 150$ cells, manual cell quantification, Student-t test) than in A549 parental cells (Fig. 4B). Yet, the main localization of YAP did not significantly differ between parental and resistant HCC827 cancer cells ($p = 0,6$; $n = 150$ cells; paired t-test) (Fig. 4B).

YAP/TEAD transcription activity is inhibited by IV#6

To characterize IV#6's effect, we performed luciferase reporter assays and analyzed YAP nuclear immunofluorescence staining in in the compound's presence or absence. YAP activity, was significantly decreased in the presence of IV#6 in A549 cells ($p = 0.0156$ for parental and resistant A549 cell line, $n = 7$; Wilcoxon test) (Fig. 5A). Conversely, despite a clear trend as (shown in **Fig. 5A**), YAP activity was not significantly altered by the compound's presence in HCC827 cells ($p = 0.1250$ for parental HC827 and $p = 0.3125$ for resistant HCC827; $n = 7$, Wilcoxon test), contrasting with IV#6's effect in cells exhibiting molecular alterations of Hippo pathway genes, which show exquisite sensitivity to YAP inhibition, possibly related to the level of YAP activation (21). The IV#6 dose used was 10µM in A549 cells and 3µM in HCC827, since 10 µM was shown to be excessively toxic in the latter (data not shown), but which also could explain why the effects were weaker in HCC827 cells than in A549 cell line.

YAP localization was studied in the presence or absence of the IV#6 YAP/TEAD interaction inhibitor compound, using three independent immunofluorescence experiments, with a total of 150 nucleocytoplasmic ratio measurements in each A549 and HCC827 cell sub-clone. A significant decrease in YAP nuclear localization was observed for cells treated with the inhibitor, 24 hours prior to labeling, in

parental as in resistant cells versus untreated cells ($p < 0.0001$ for A549 and A549R cells; $p = 0.002$ for parental HCC827 and $p = 0.0007$ for resistant HCC827 cells, Student's t-test) **(Fig. 5B).**

The YAP activity was then further measured by luciferase assay on three other cell types **(Fig. 5C).** PC-9 and H2052 lines were reported to display high YAP activity (20, 21). In both cell types, a significant decrease in the YAP activity was observed in the presence of relatively low IV#6 doses (for H2052 cell line: $p = 0.0236$, IV#6 3µM, $n = 5$, Student's t-test and for PC9 cell line: $p = 0.0156$; IV#6 3µM, $n = 7$, Wilcoxon test). PC-9 cell line, with oncogenic EGFR mutation, was recently reported to exhibit YAP/TEAD signaling activation in line with a TP53 gain of function mutation, which results in mevalonate pathway activation, inducing cytoskeleton rearrangements *via* Rho activation, and ultimately YAP nuclear translocation (21). H2052 exhibits two mutations in genes of the Hippo pathway, leading to YAP nuclear accumulation and activation (20). This YAP pharmacological inhibition was not found in a third EGFR-mutated cell model, the HCC4006 cell line ($p = 0.1250$; IV#6 1.5µM, $n = 4$, Wilcoxon test) (Fig. 5C).

YAP/TEAD transcriptional signature in parental and paclitaxel-resistant cells

Differential transcriptomic analysis between parental and resistant A549 cells revealed resistant cells to display an overexpression of YAP/TEAD target mRNAs as compared to the parental cell line (analysis using Metascape and EnrichR) (Fig. 6A). Similar pathways were highly represented in both cell lines, including cell cycle, MYC target, oxidative phosphorylation, and RNA metabolism. We assessed the expression of YAP/TEAD target genes by constructing a 42-genes YAP/TEAD signature (Fig. 6B **left**), based on our data mining from published literature, only selecting YAP/TEAD target genes by CHIPseq defined by at least two different teams, and two different cell types (7, 37, 38). Such list comprised well-known targets, some of which being Hippo pathway members (AJUBA, FAT1, FRMD6, TEAD1/4, STK3/MST2, STK4/MST1 (Hippo), SCRIB, LATS2, WWTR1/TAZ, WWC1/Kibra), while others were classical targets responsible the YAP/TEAD's signaling pleïotropic effects, including AXL, AREG, CCND1, BIRC5/survivin. We compared mean expression and mean z-score of individual genes as well as the whole signature in our two cell lines A549 and A549R, either treated or not, with the YAP/TEAD inhibitor (Fig. 6B **right**). GSEA analysis, based on the Broad Hallmark geneSet, confirmed the significant down-regulation of these YAP/TEAD target genes in resistant A549 cells, after treatment with the compound ($p = 0.05$ mean expression; $p = 0.037$ Z-score). Despite an objective trend towards reduced YAP/TEAD targets expression in parental cells, following treatment with the compound, the results did not reach statistical significance ($p = 0,7$ for mean expression; $p = 0,5$ for Z-score). This suggested that pharmacological YAP/TEAD inhibition displayed specifically dramatic effects only on cells with basal high-level YAP activation, including the paclitaxel-resistant A549. Individual classical transcriptional YAP target genes, namely CTGF and CYR61, were also up-regulated in resistant cells as compared with parental cells, with a decreased expression upon IV#6 in both resistant and parental A549 cells (p-value < 0.05) (Fig. 6C).

IV#6 compound partly restores chemo-sensitivity to Paclitaxel

Figure 7A displays the IC_{50} curves of paclitaxel from the four independent experiments combined, illustrating the pharmacological inhibitor effect in restoring chemotherapy sensitivity in resistant cells (purple curve). Calculation of the areas under the curve (Fig. 7B) confirmed that adding IV#6 (10µM) significantly reduced the area under the curve in resistant A549 cells ($p = 0.02$; $n = 4$; Mann Whitney test), thereby increasing the sensitivity of these cells cultured in 2D, to paclitaxel. This difference was not observed in parental A549 cells, which remained sensitive to paclitaxel (Fig. 7C).

To further demonstrate the Inventiva™-supplied anti-YAP compound ability to restore sensitivity to the cytotoxic agent paclitaxel, we moved to a "tumor on chip" 3D micro-fluidic culture experimental system (Fig. 8A). We started with the A549 lung cancer cell line model, which revealed some clear YAP signaling activation, shown in our transcriptomic data. We therefore incubated A549 cells embedded in collagen with a medium containing different drugs at different concentrations, as well as a green apoptosis reporter (Cell Event Caspase 3/7). The microfluidic chips were imaged under the microscope for 72h. We used STAMP software to quantify apoptosis events over time (24). Parental and resistant A549 cells were treated either with 100 nM paclitaxel alone, IV#6 compound at 20 µM, or 100nM paclitaxel and 20µM IV#6 combined. DMSO and 20 nM paclitaxel constituted the control condition for A549 cells and paclitaxel-resistant A549R cells respectively, since the latter are routinely grown in presence of low-dose 20 nM paclitaxel.

In parental cells, combining IV#6 and paclitaxel, resulted in a slightly higher effect on cell death than the control ($p = 0.04$, 2-way Anova, $n = 3$) (Fig. 8B **left**). In resistant A549 cells, combining 20µM IV#6 and 100nM paclitaxel, significantly and substantially increased cell death, versus the control conditions ($p = 0.02$, 2way Anova, $n = 3$) and the 100nM paclitaxel single-therapy ($p = 0.04$, 2-way Anova, $n = 3$) (Fig. 8B **right**). This result indicated that inhibition of YAP by the IV#6compound under 3D chip culture conditions, at least partly restored paclitaxel chemo-sensitivity in resistant cells, supporting the YAP-TEAD pathway's role in paclitaxel resistance of A549 lung cancer cells.

We additionally studied the compound effect in combination with paclitaxel on cancer cells from fresh tumors, from lung cancer patients operated on at Bichat Hospital, providing herein the example of a 70-year-old smoker, who underwent right upper lobectomy for a 10% PD-L1-expressing lung adenocarcinoma, without molecular addictive driver alteration. For this experiment, we used DRAQ7 as a fluorescence general death-induced marker to monitor all-cause cell death. To this end we manually counted dying cells as a function of time. Figure 8C illustrates the cell death rate per 10 hours (left panel), and the cumulative cell death rate (right panel), over 48 hours. The anti-YAP/TEAD compound alone was not toxic at 5 and 10µM in this experiment (red and magenta curves), while adding paclitaxel alone (200 nM, green curve) led to cell death, as expected. Combining paclitaxel and 10µM IV#6 (but not 5µM), thus likely induced a higher effect with a significantly greater increase in cell death versus paclitaxel alone. Such preliminary data actually indicated that patient-derived tumor-on chips consisted of an efficient strategy to investigate chemotherapy combinations with YAP inhibitors, and to address the complexity of patient response heterogeneity.

Discussion

Using pharmacological YAP/TEAD interaction inhibitors we have provided some clues concerning the involvement of YAP signaling in acquired resistance to paclitaxel in lung cancer cells, seeking to target or block the Hippo/YAP signaling pathway to restore chemo-sensitivity or prevent acquired resistance in lung cancer patients, who received paclitaxel in combination with carboplatin, and often with an anti-PD-1 monoclonal antibody. Inventiva™ provided us with a series of compounds isolated in a high throughput screen for drugs able to disrupt the interaction of YAP with its main target, the TEAD transcription factor. While the chemical structure of such compounds is still confidential, we have generated preliminary data showing that these drugs could actually act by inhibiting YAP signaling, on account of inhibiting biological properties attributed to TEAD transcriptional program: *i)* these drugs were able to inhibit 2D migration of lung A549 and mesothelioma H2052 cancer cells, with activated YAP due to their genetic background, but without altering cell survival at a 20 µM dose. Such effect was fully reminiscent with what we previously described by knockdown RASSF1A gene in bronchial cells, thereby up-regulating YAP (15); *ii)* these compounds were also able to induce YAP nuclear exit, their efficacy being lower in immortalized, not-tumorigenic mesothelial cells devoid of basal YAP activation; *iii)* by means of YAP pharmacological inhibition using the two most promising compounds, as based on these two first assays (*i.e.*, cell migration and YAP nucleocytoplasmic shuttling),, we were also able to recap the synthetic lethality induced by combining trametinib MEK inhibition with the YAP inhibitor, in K-RAS, MAP-K activated A549 cell line, as did T. Bivona's group while using RNA interference to deplete YAP (27). *iv)* taking advantage of the YAP signaling involvement in EMT promotion, we eventually demonstrated that IV#6 was able to partly revert the TGFβ−ινδυχεδ EMT in A549 lung cancer cells. Collectively, our data supported that Inventiva™-isolated compounds exerted anti-YAP effects, given that they inhibited four well-known consequences of YAP activation in lung cancer (15, 20, 27).

We additionally addressed the issue of YAP contribution to paclitaxel resistance using two lung cancer cell lines couples, the A549 and HCC8277 parental cells, and their counterpart with acquired resistance to paclitaxel upon long-term culture with sub-lethal paclitaxel doses. While the HCC827 couple did not reveal any significant nuclear staining differences between sensitive and resistant cells, we found a much higher nuclear YAP content in A549R cells, the "YAP-activated" status of which has been well established in literature (15, 27). The HCC827 cell line despite having an EGFR oncogenic mutation, has never been described as a "YAP-activated" cell model to date. Using a transactivation luciferase reporter assay (28), we showed that the YAP inhibitor IV#6 could significantly lower TEAD transcriptional activity, demonstrating the direct effect of such compound on TEAD activity. This latter activity is probably accounted for by disrupting YAP interaction with TEAD. A further step demonstrated the ability of this YAP/TEAD pharmacological inhibitor to lower nuclear YAP staining in both paclitaxel-sensitive and paclitaxel-resistant cells. Yet, this reduction was solely found in cells with activated YAP, as evidenced by the luciferase assay, *i.e.* lung cancer A549 cell lines couple and PC-9, or mesothelioma H2052 cells.

To support the activation of YAP/TEAD transcriptional activity in A549 model, we performed whole-exome RNAseq of both cells lines thereby demonstrating the enrichment of a YAP 42-genes signature, in

both A549 and A549R sub-clones, the latter showing higher increase as compared with parental cells. Furthermore, by treating these cells with IV#6 YAP/TEAD inhibitor, we demonstrated that the whole YAP/TEAD signature was down-regulated, as individual classical YAP targets (CYR61, CTGF). By treating these two sub-clones, with either paclitaxel alone or IV#6 plus paclitaxel doublet, we confirmed that there were actually two logs of difference in paclitaxel IC_{50} values between the sensitive and resistant sub-clones, while demonstrating a significant decrease in paclitaxel IC_{50} values of the A549R paclitaxel resistant clone. Based on these findings, the YAP/TEAD inhibition could, at least to some extent, revert paclitaxel resistance in A549 lung cancer cells.

Such data must be put in perspective with the reported role of YAP/TAZ in the acquired resistance to RAF or EGFR inhibitors (20, 21, 39, 40). Indeed, these anti-BRAF treatments were shown to induce actin cytoskeleton remodeling and thus promote YAP activation via Rho-mediated inhibition of LATS1/2, in BRAF-mutated melanoma cells (20, 21). However, our comparative transcriptomic analyses on parental and resistant A549 cells also demonstrated that the transcriptome was massively deregulated in resistant cells, with other signaling pathways differentiating these two cell sub-clones, in addition to YAP/TEAD. It is possible that YAP inhibition could only partly revert chemo-resistance, while several other mechanisms, yet to be uncovered, could also contribute to such chemo-resistance.

In particular, the possible participation of Notch, Hedgehog and Wingless-type protein (Wnt) pathways, widely described in the literature for their contribution to chemo-resistance should be mentioned here (29, 30), Indeed Notch2 was recently revealed as a *bona fide* YAP/TEAD transcriptional target in small-cell lung cancer cells (31). YAP was actually shown to drive chemo-resistance in such cells, while additionally inducing the emergence of a non-neuroendocrine phenotype. Of note, our transcriptomic analysis of A549R cells also found an enrichment of the genes belonging to these pathways, whereas it is still unknown whether this was due to YAP activation or not.

One important asset of our work is the employment of a 3D microfluidic cell culture chip. Major inconsistencies between drug sensitivity determined on 2D cell culture, and clinical drug efficacy have been claimed. PDX models emerged, but need weeks to be stably established, which actually does not meet the clinical requirements (32). Moreover PDX are not adapted to immunotherapy since using immune-deficient mice (32). More recently, spheroids and cell culture 3D on-chip systems have emerged. Both recapitulated 3D cell cultures conditions, which were shown to provide more consistent results in drug efficacy assays, while better correlating with clinical observations. Both approaches could result in exploitable results within a short time period, ranging from four to 15 days, which is considered compatible with clinical needs. Microfluidic systems allow for low quantities of cells (1,000). Using cell death fluorescent markers, they also allow for semi-automated cell death quantification, on account of cell imaging analysis algorithms(24). These could be instrumental in reconstituting a more physiological, still imperfect, tumor microenvironment, by co-culturing cancer-associated fibroblasts (18) and autologous immune cells (24), which are all embedded in the same collagen polymerized matrix (33–35). We employed a very simple microfluidic chip to reproduce the cumulative effect of YAP/YEAD pharmacological inhibitor added to paclitaxel in sensitive and resistant lung cancer A549 cell lines.

Moreover, we sought to develop such systems in order to obtain a rapid response concerning the efficacy of drugs, in individual patients, and for guiding their treatment choice, including immune checkpoint inhibitors. Indeed, the system could be rendered fully immune-competent while using autologous T-cells purified from the same tumor (24, 36). Accordingly, as a proof of concept, we were able to generate such a cell culture system from a patient who underwent lung cancer surgical resection. By doing so, we succeeded in assessing the efficacy of IV#6 combined with paclitaxel, demonstrating a promising cytotoxic effect versus paclitaxel given alone. Further experiments with cells originating from several additional patients are still on-going, using chemotherapy and immune checkpoint inhibition (Veith I *et al*. submitted manuscript). Given that the YAP/TEAD transcriptional program contains multiple genes involved in immune response to cancer, resulting in immune cells recruitment and activation (CXCL5, CXCL2, SMAD2/3, CYR61, IL2, IL12A, IL1B, JAK2...), immune-suppressive CAF recruitment (CTGF, DPP4, GAS6, AXL), and or T-cell exhaustion (PD-L1, CTLA-4) (7, 37, 38), the pharmacological inhibition of YAP/TEAD could result in the potentiation of immune checkpoint inhibitor treatment. Further preclinical studies with our lung cancer on chip microfluidic device are thus warranted, using patients' fresh autologous cells.

Conclusions

While Hippo/YAP signaling pathway has been involved in the acquired resistance to EGFR or B-RAF tyrosine kinase inhibitors in lung cancer, we now provide evidence that acquired resistance to paclitaxel could also involve increased YAP activity. By using YAP/TEAD pharmacological inhibition we showed that YAP/TEAD inhibition has the potential to revert chemotherapy resistance. We provide data showing that cells exhibiting high YAP/TEAD transcriptional activity could show exquisite sensitivity to such pharmacological inhibitors, paving the way for future clinical development. Finally, we report the use of an original patient-derived 3D microfluidic cell culture system, to assay *ex-vivo* such inhibitors in combination with chemotherapy.

Declarations

Acknowledgements and Fundings

This work was funded by the National Agency for Research grant #ANR 2017 'Hippocure' (G. Zalcman & Inventiva™ pharma company), the ARC Foundation for cancer research grant #PGA RF20180206991 (MC Parrini), and ITMO INSERM grant '3R', #19CR046-00 (MC Parrini & S. Descroix). We are thankful for excellent discussions and intellectual interchange to Dr. Martine Barth, PhD (from InventivaÔ) and Dr. Anne Soude, PhD (from Inventiva™).

References

1. Global Cancer Observatory [Internet]. [cité 5 oct 2022]. Disponible sur: https://gco.iarc.fr/.

2. Nguyen CDK, Yi C. YAP/TAZ Signaling and Resistance to Cancer Therapy. Trends Cancer. 2019;5(5):283–96.
3. Volk-Draper L, Hall K, Griggs C, Rajput S, Kohio P, DeNardo D, et al. Paclitaxel therapy promotes breast cancer metastasis in a TLR4-dependent manner. Cancer Res. 2014;74(19):5421–34.
4. Han ZX, Wang HM, Jiang G, Du XP, Gao XY, Pei DS. Overcoming paclitaxel resistance in lung cancer cells via dual inhibition of stathmin and Bcl-2. Cancer Biother Radiopharm. 2013;28(5):398–405.
5. Orr GA, Verdier-Pinard P, McDaid H, Horwitz SB. Mechanisms of Taxol resistance related to microtubules. Oncogene. 2003;22(47):7280–95.
6. Monzó M, Rosell R, Sánchez JJ, Lee JS, O'Brate A, González-Larriba JL, et al. Paclitaxel resistance in non-small-cell lung cancer associated with beta-tubulin gene mutations. J Clin Oncol. 1999;17(6):1786–93.
7. Zhao B, Li L, Lei Q, Guan KL. The Hippo-YAP pathway in organ size control and tumorigenesis: an updated version. Genes Dev. 2010;24(9):862–74.
8. Avruch J, Zhou D, Fitamant J, Bardeesy N, Mou F, Barrufet LR. Protein kinases of the Hippo pathway: regulation and substrates. Semin Cell Dev Biol. 2012;23(7):770–84.
9. Battilana G, Zanconato F, Piccolo S. Mechanisms of YAP/TAZ transcriptional control. Cell Stress. 2021;5(11):167–72.
10. Wang Y, Dong Q, Zhang Q, Li Z, Wang E, Qiu X. Overexpression of yes-associated protein contributes to progression and poor prognosis of non-small-cell lung cancer. Cancer Sci. 2010;101(5):1279–85.
11. de Fraipont F, Levallet G, Creveuil C, Bergot E, Beau-Faller M, Mounawar M, et al. An apoptosis methylation prognostic signature for early lung cancer in the IFCT-0002 trial. Clin Cancer Res. 2012;18(10):2976–86.
12. Zanconato F, Cordenonsi M, Piccolo S. YAP/TAZ at the Roots of Cancer. Cancer Cell. 2016;29(6):783–803.
13. Tang Z, Ma Q, Wang L, Liu C, Gao H, Yang Z, et al. A brief review: some compounds targeting YAP against malignancies. Future Oncol. 2019;15(13):1535–43.
14. Sebio A, Lenz HJ. Molecular Pathways: Hippo Signaling, a Critical Tumor Suppressor. Clin Cancer Res. 2015;21(22):5002–7.
15. Dubois F, Keller M, Calvayrac O, Soncin F, Hoa L, Hergovich A et al. RASSF1A Suppresses the Invasion and Metastatic Potential of Human Non-Small Cell Lung Cancer Cells by Inhibiting YAP Activation through the GEF-H1/RhoB Pathway. Cancer Res;76(6):1627–40.
16. Keller M, Dubois F, Teulier S, Martin APJ, Levallet J, Maille E, et al. NDR2 kinase contributes to cell invasion and cytokinesis defects induced by the inactivation of RASSF1A tumor-suppressor gene in lung cancer cells. J Exp Clin Cancer Res. 2019;38(1):158.
17. Sontheimer-Phelps A, Hassell BA, Ingber DE. Modelling cancer in microfluidic human organs-on-chips. Nat Rev Cancer. 2019;19(2):65–81.

18. Nguyen M, De Ninno A, Mencattini A, Mermet-Meillon F, Fornabaio G, Evans SS, et al. Dissecting Effects of Anti-cancer Drugs and Cancer-Associated Fibroblasts by On-Chip Reconstitution of Immunocompetent Tumor Microenvironments. Cell Rep. 2018;25(13):3884–3893e3.
19. Portillo-Lara R, Annabi N. Microengineered cancer-on-a-chip platforms to study the metastatic microenvironment. Lab Chip. 2016;16(21):4063–81.
20. Maille E, Brosseau S, Hanoux V, Creveuil C, Danel C, Bergot E, et al. MST1/Hippo promoter gene methylation predicts poor survival in patients with malignant pleural mesothelioma in the IFCT-GFPC-0701 MAPS Phase 3 trial. Br J Cancer. 2019;120(4):387–97.
21. Esposito D, Pant I, Shen Y, Qiao RF, Yang X, Bai Y, et al. ROCK1 mechano-signaling dependency of human malignancies driven by TEAD/YAP activation. Nat Commun. 2022;13(1):703.
22. Soude A, Barth M, Bocart S, Thoreau F, Mandry E, Contal S, et al. Abstract A129: Generation of YAP-TEAD Protein-Protein Interaction (PPI) inhibitors for the treatment of cancer. Mol Cancer Ther. 2015;14(12Supplement2):A129.
23. Deforet M, Parrini MC, Petitjean L, Biondini M, Buguin A, Camonis J, et al. Automated velocity mapping of migrating cell populations (AVeMap). Nat Methods. 2012;9(11):1081–3.
24. Veith I, Mencattini A, Picant V, Serra M, Leclerc M, Comes MC, et al. Apoptosis mapping in space and time of 3D tumor ecosystems reveals transmissibility of cytotoxic cancer death. PLoS Comput Biol. 2021;17(3):e1008870.
25. Corgnac S, Damei I, Gros G, Caidi A, Terry S, Chouaib S, et al. Cancer stem-like cells evade CD8 + CD103 + tumor-resident memory T (TRM) lymphocytes by initiating an epithelial-to-mesenchymal transition program in a human lung tumor model. J Immunother Cancer. 2022;10(4):e004527.
26. Biondini M, Duclos G, Meyer-Schaller N, Silberzan P, Camonis J, Parrini MC. RalB regulates contractility-driven cancer dissemination upon TGFβ stimulation via the RhoGEF GEF-H1. Sci Rep. 2015;5:11759.
27. Lin L, Sabnis AJ, Chan E, Olivas V, Cade L, Pazarentzos E, et al. The Hippo effector YAP promotes resistance to RAF- and MEK-targeted cancer therapies. Nat Genet. 2015;47(3):250–6.
28. Dupont S, Morsut L, Aragona M, Enzo E, Giulitti S, Cordenonsi M, et al. Role of YAP/TAZ in mechanotransduction. Nature. 2011;474(7350):179–83.
29. Stewart DJ. Tumor and host factors that may limit efficacy of chemotherapy in non-small cell and small cell lung cancer. Crit Rev Oncol Hematol sept. 2010;75(3):173–234.
30. Stewart DJ. Wnt Signaling Pathway in Non–Small Cell Lung Cancer. J Natl Cancer Inst;106(1). available on https://academic.oup.com/jnci/article/106/1/djt356/2518008.
31. Wu Q, Guo J, Liu Y, Zheng Q, Li X, Wu C, et al. YAP drives fate conversion and chemoresistance of small cell lung cancer. Sci Adv. 2021;7(40):eabg1850.
32. Decaudin D. Primary human tumor xenografted models ('tumorgrafts') for good management of patients with cancer. Anticancer Drugs oct. 2011;22(9):827–41.

33. Huh D, Matthews BD, Mammoto A, Montoya-Zavala M, Hsin HY, Ingber DE. Reconstituting organ-level lung functions on a chip. Science. 2010;328(5986):1662–8.
34. Benam KH, Villenave R, Lucchesi C, Varone A, Hubeau C, Lee HH, et al. Small airway-on-a-chip enables analysis of human lung inflammation and drug responses in vitro. Nat Methods. 2016;13(2):151–7.
35. Jain A, Barrile R, van der Meer AD, Mammoto A, Mammoto T, De Ceunynck K, et al. Primary Human Lung Alveolus-on-a-chip Model of Intravascular Thrombosis for Assessment of Therapeutics. Clin Pharmacol Ther. 2018;103(2):332–40.
36. Mencattini A, Lansche C, Veith I, Erbs P, Balloul JM, Quemeneur E, et al. Direct imaging and automatic analysis in tumor-on-chip reveal cooperative antitumoral activity of immune cells and oncolytic vaccinia virus. Biosens Bioelectron. 2022;215:114571.
37. Stein C, Bardet AF, Roma G, Bergling S, Clay I, Ruchti A, et al. YAP1 Exerts Its Transcriptional Control via TEAD-Mediated Activation of Enhancers. PLoS Genet. 2015;11(8):e1005465.
38. Zanconato F, Forcato M, Battilana G, Azzolin L, Quaranta E, Bodega B, et al. Genome-wide association between YAP/TAZ/TEAD and AP-1 at enhancers drives oncogenic growth. Nat Cell Biol. 2015;17(9):1218–27.
39. Hsu PC, You B, Yang YL, Zhang WQ, Wang YC, Xu Z, et al. YAP promotes erlotinib resistance in human non-small cell lung cancer cells. Oncotarget. 2016;7(32):51922–33.
40. Fan PD, Narzisi G, Jayaprakash AD, Venturini E, Robine N, Smibert P, et al. YES1 amplification is a mechanism of acquired resistance to EGFR inhibitors identified by transposon mutagenesis and clinical genomics. Proc Natl Acad Sci. 2018;115(26):E630–38.

Figures

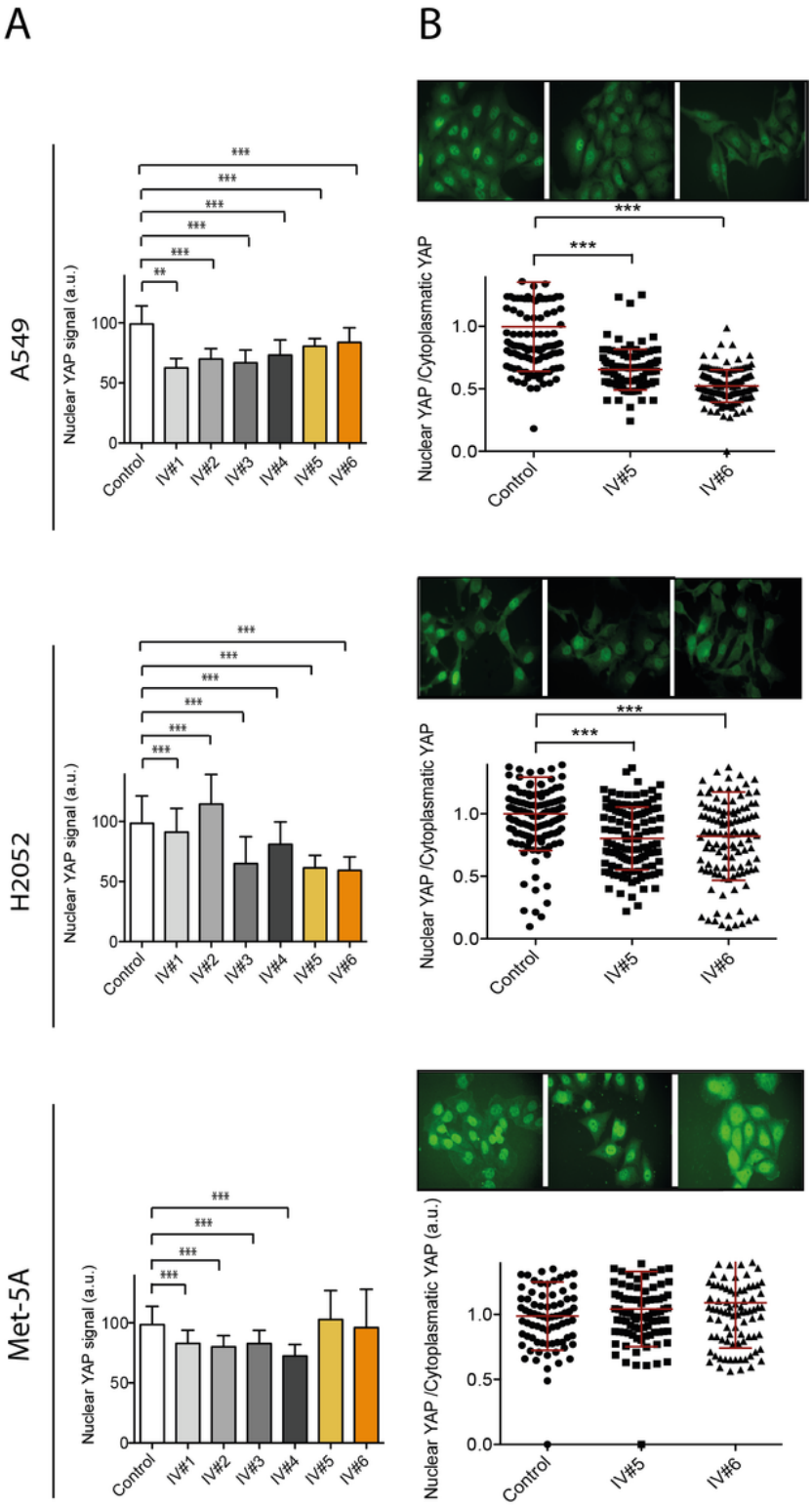

Figure 1

Figure legend not available with this version.

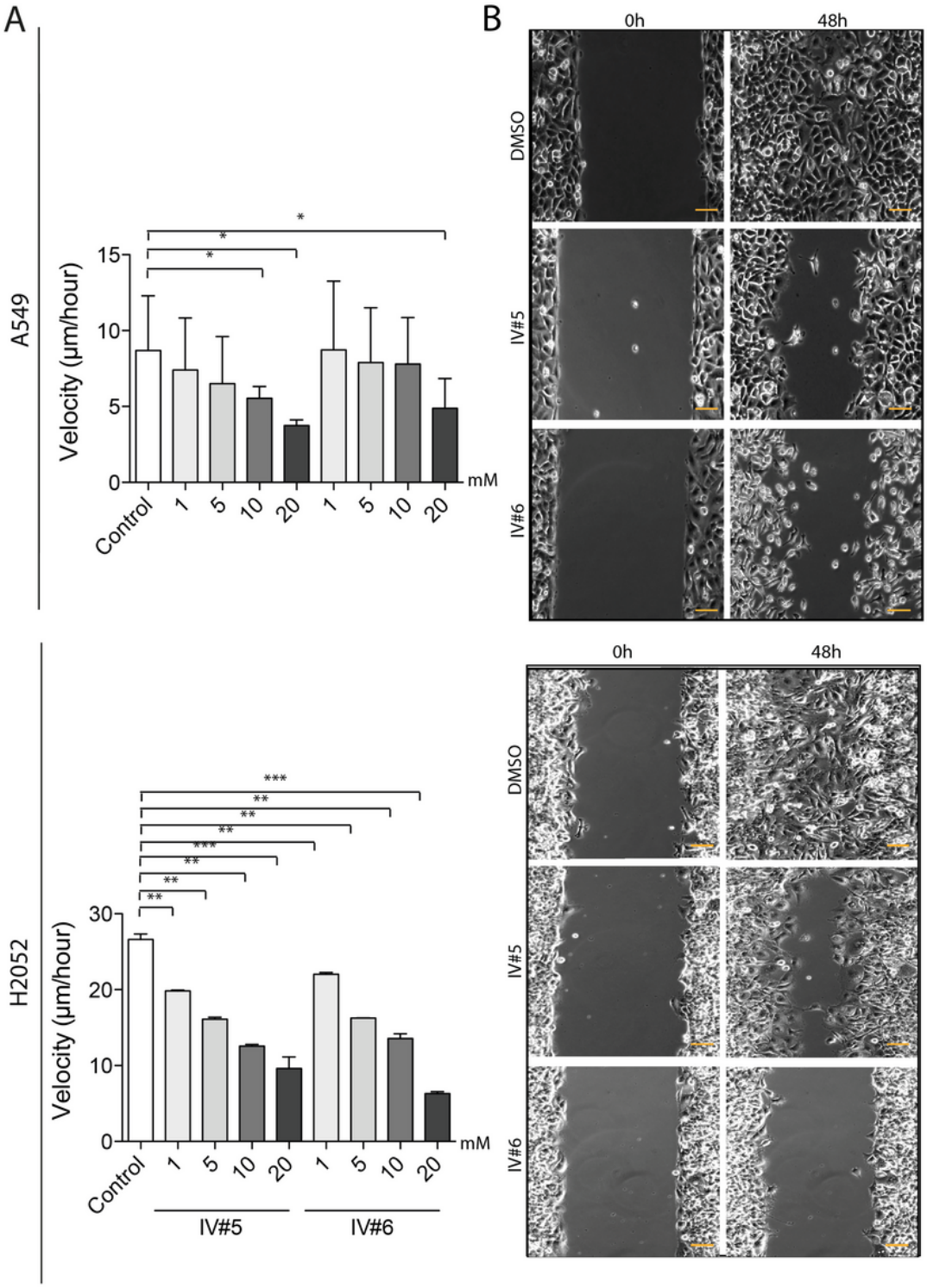

Figure 2

Figure legend not available with this version.

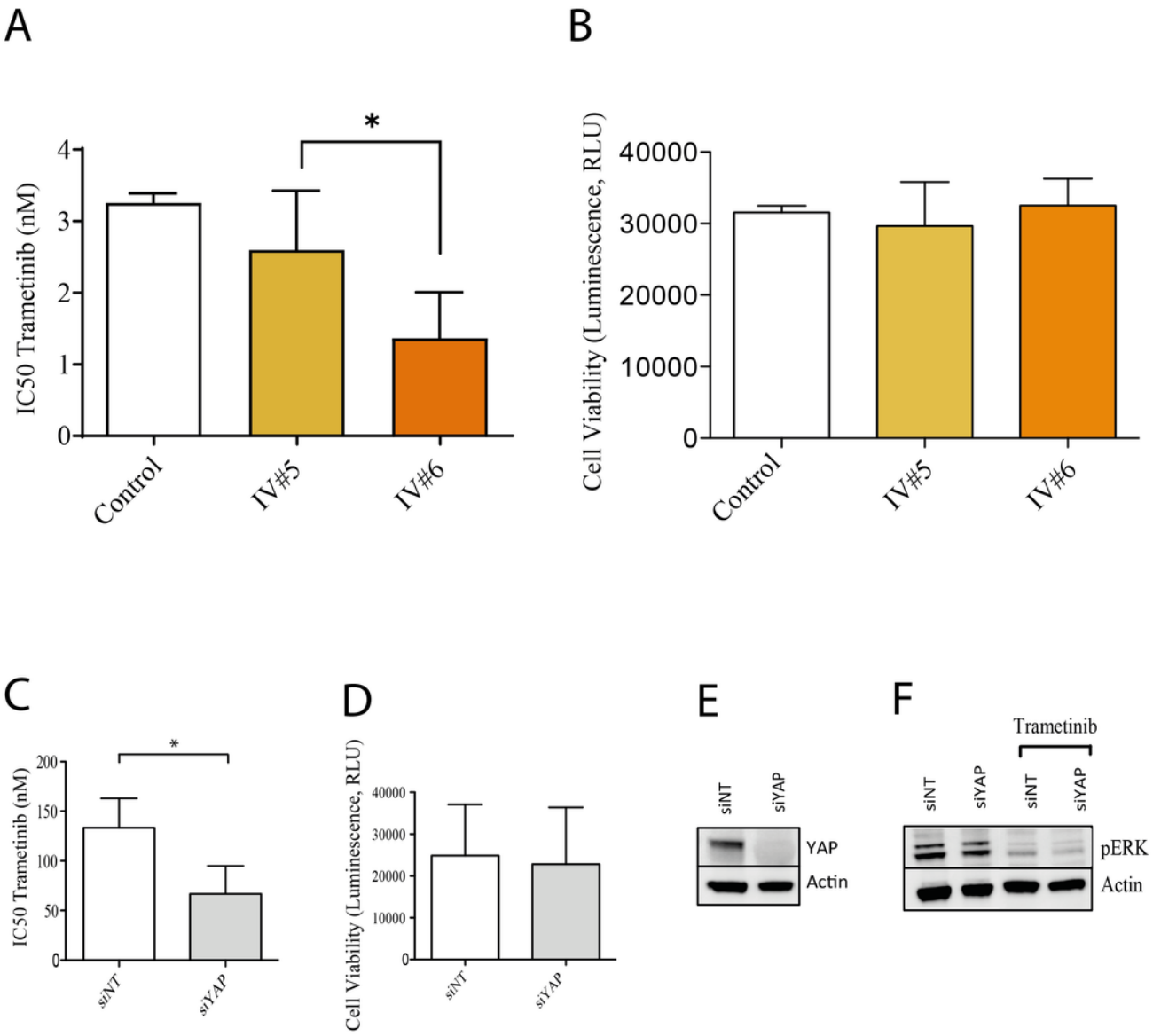

Figure 3

Figure legend not available with this version.

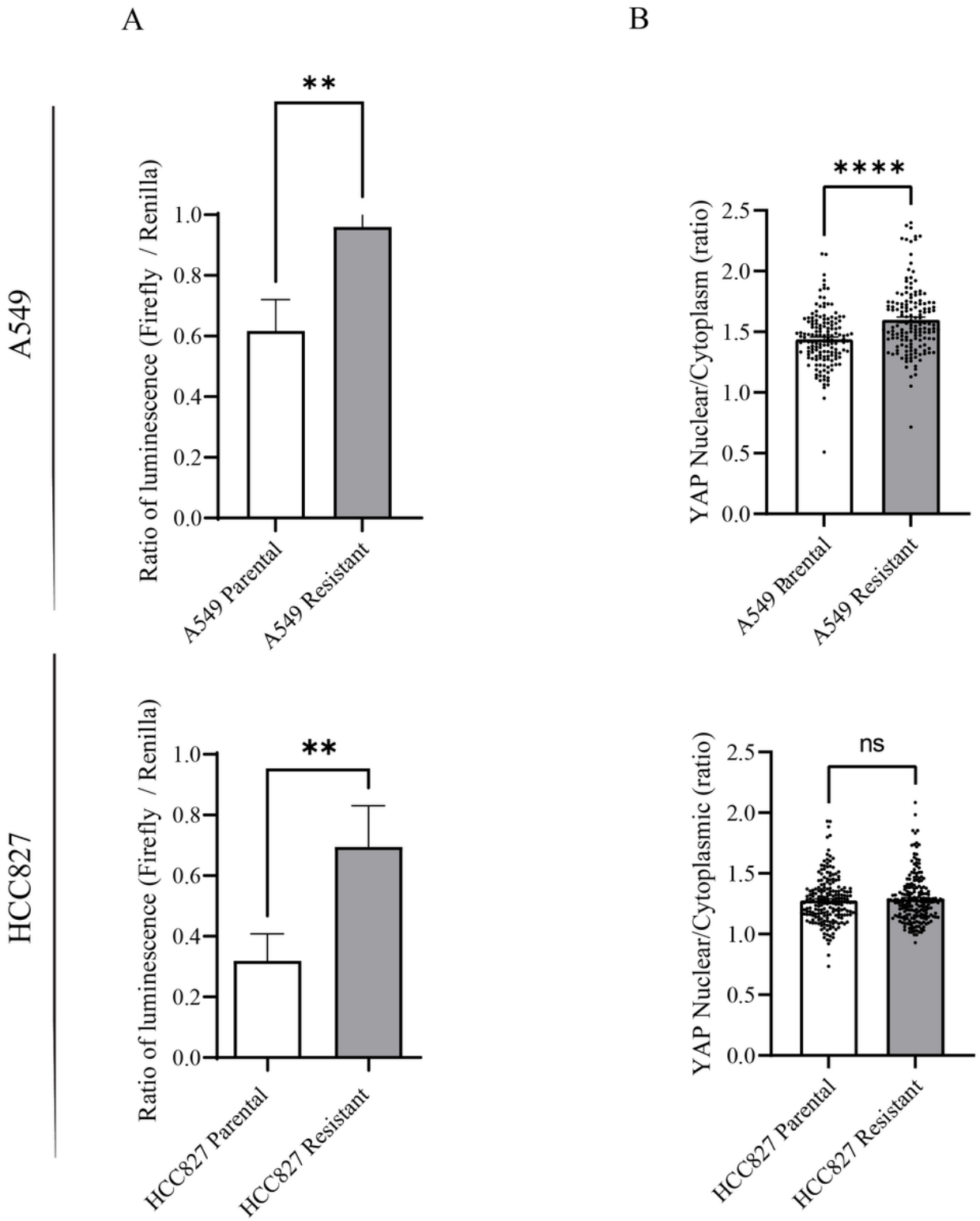

Figure 4

Figure legend not available with this version.

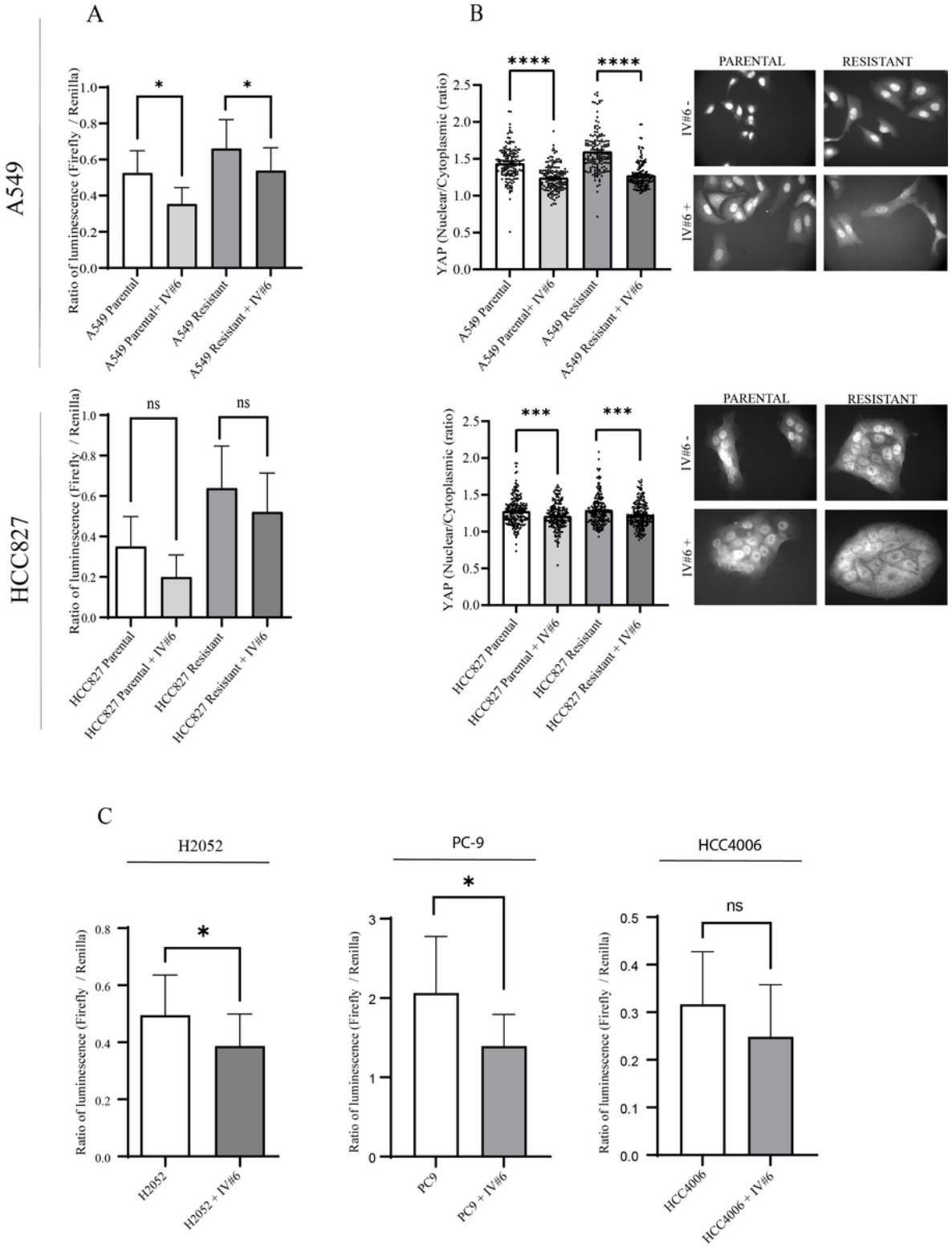

Figure 5

Figure legend not available with this version.

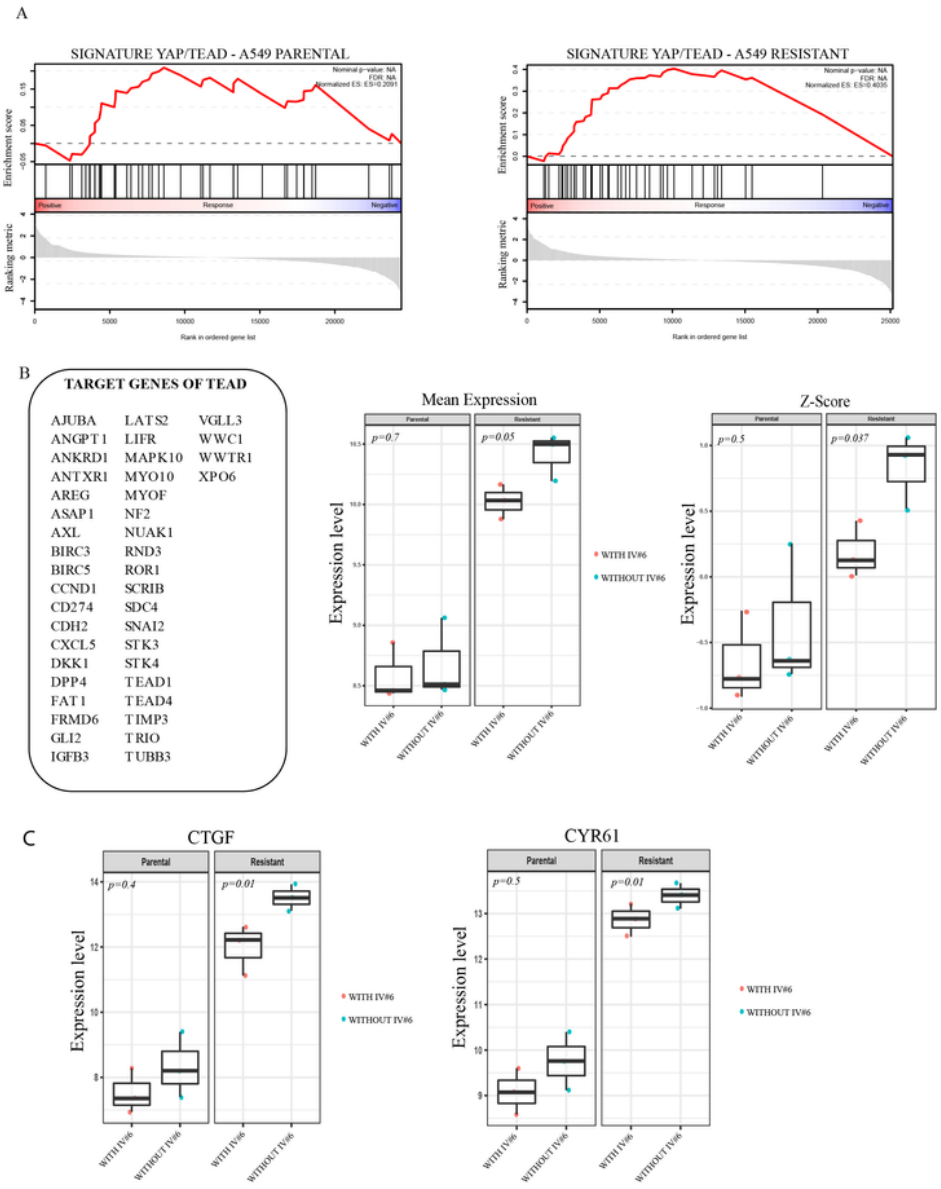

Figure 6

Figure legend not available with this version.

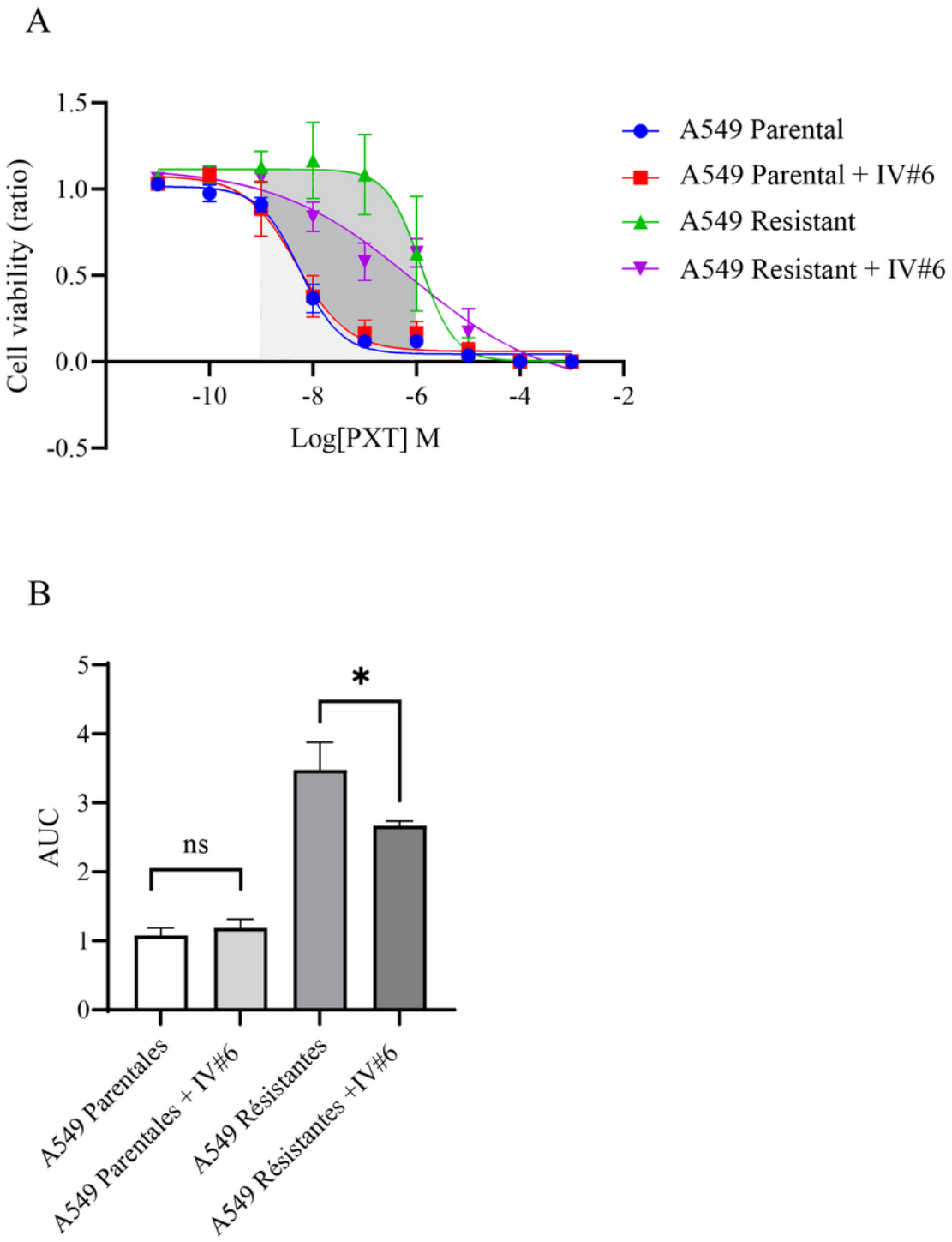

Figure 7

Figure legend not available with this version.

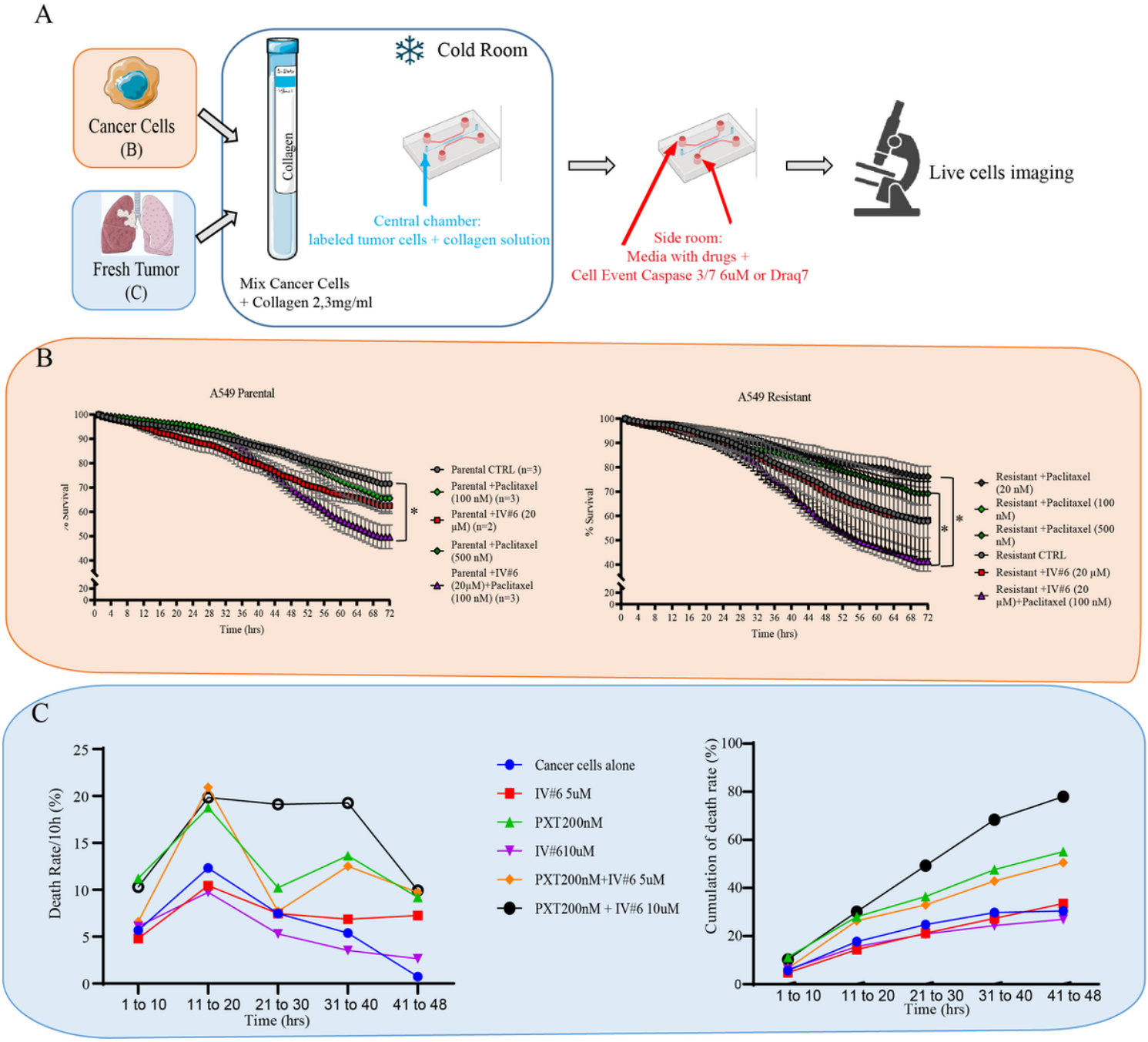

Figure 8

Figure legend not available with this version.

Supplementary Files

This is a list of supplementary files associated with this preprint. Click to download.

- Supplementary1YAPinhibdecreasecellvelocity.png
- Supplementary2EMT.png